Lens Distortion Correction In Expensive Lens Compared To Cheap Lens

A Report submitted

in partial fulfillment for the Degree of

Bachelor of Technology

in

Mechanical Engineering

by

Vedant Nitin Dahake (2020BME036)

Under the guidance of

Dr. Jeet P. Patil

2023-24

Department of Mechanical Engineering

Shri Guru Gobind Singhji Institute of Engineering and Technology

(SGGSIE&T), Vishnupuri, Nanded-431606, MH, India

CERTIFICATE

This is to certify that the project report entitled **Lens Distortion Correction In Expensive Lens Compared To Cheap Lens** submitted by **Vedant Nitin Dahake (2020BME036)** to Shri Guru Gobind Singhji Institute of Engineering and Technology (SGGSIE&T), Vishnupuri Nanded, in partial fulfillment for the award of the degree of **B. Tech in Mechanical Engineering** is a bona-fide record of project work carried out by him under my supervision. The contents of this report, in full or in parts, have not been submitted to any other Institution or University for the award of any degree or diploma.

Dr. Jeet P. Patil

Supervisor

Department of Mechanical Engineering

Vishnupuri, Nanded

May 2024

HOD

Department of Mechanical Engineering

EXAMINERS APPROVAL SHEET

This is to certify that the project report entitled **Lens Distortion Correction In Expensive Lens Compared To Cheap Lens** submitted by **Vedant Nitin Dahake (2020BME036)** to Shri Guru Gobind Singhji Institute of Engineering and Technology (SGGSIE&T), Vishnupuri Nanded, in partial fulfillment for the award of the degree of **B. Tech in Mechanical Engineering**; is hereby approved for the award of degree.

External Examiner

Internal Examiner

Superviosor (s)

DECLARATION

I, declare that this project report titled **Lens Distortion Correction In Expensive Lens Compared To Cheap Lens** submitted in partial fulfillment of the degree of **B. Tech in Mechanical Engineering** is a record of original work carried out by me/us under the supervision of **Dr. Jeet P. Patil**, and has not formed the basis for the award of any other degree or diploma, in this or any other Institution or University. In keeping with the ethical practice in reporting scientific information, due acknowledgements have been made wherever the findings of others have been cited.

Vedant Nitin Dahake (2020BME036)

Vishnupuri, Nanded-431606

25th May 2024

ACKNOWLEDGMENTS

I take this opportunity to thank Dr. Manesh B. Kokare, Director SGGSIE&T, Dr. Sourabh S. Jogee, Head of Mechanical Engineering Department and other faculty members who helped in preparing the guidelines.

I extend my sincere thanks to one and all of SGGSIE&T family for the completion of this document on the project report format guidelines.

Vedant Nitin Dahake (2020BME036)

ABSTRACT

Lens distortion will cause errors in the measurement of deformation by digital image correlation when using a microscope at high magnification for image recording. To improve the measurement accuracy of 2D digital image correlation, lens distortion was detected by rigid-body translation tests for a micro speckle pattern using DIC calculation. Based on the first-order radial distortion model, the coefficients for the lens distortion were determined using the least-squares method. Then, the displacement fields without lens distortion were obtained, and accurate measurements were achieved even for images that were deformed by lens distortion. The results demonstrate that the average error in the displacement fields decreases by 20% for expensive lens, distortion correction by rigid-body translation tests of a micro speckle pattern using DIC calculation. The experimental results verify that digital image correlation is a powerful tool for micro-scale deformation measurement using a microscope at high magnification as long as one correct for lens distortion.

TABLE OF CONTENTS

CERTIFICATE vi

EXAMINERS APPROVAL SHEET vii

DECLARATION viii

ACKNOWLEDGMENTS viv

ABSTRACT v

ABBREVIATIONS x

CHAPTER 1 INTRODUCTION 1

1.1. INTRODUCTION TO DIC 1

1.2. DISTORTIONS AND ITS EFFECTS 2

1.3. OBJECTIVES 3

CHAPTER 2 LITERATURE REVIEW 4

2.1. INTRODUCTION 4

2.2. EARLY APPLICATIONS AND METHODOLOGICAL DEVELOPMENTS 4

2.3. INNOVATIONS IN DIC TECHNOLOGY 4

2.4. APPLICATION IN VARIOUS MATERIALS AND CONDITIONS 5

2.5. ADDRESSING METHODOLOGICAL CHALLENGES 5

2.6. RECENT DEVELOPMENTS AND FUTURE DIRECTIONS 5

CHAPTER 3 DISTORTION CORRECTION BY MEASURING RIGID BODY DISPLACEMENT 6

3.1. DISTORTION MODEL 6

3.2. DISTORTION CORRECTION 7

CHAPTER 4 SAMPLE PREPARATION 10

CHAPTER 5 EXPERIMENTAL SETUP 11

5.1. RIGID BODY IN-PLANE TRANSLATION TEST FOR EXPENSIVE LENS 11

5.2. RIGID BODY IN-PLANE TRANSLATION TEST FOR CHEAP LENS 112

5.3. TEST TO COMPARE DIC TO FEM ANALYSIS (DIC Tester) 12

CHAPTER 6 RESULTS AND DISCUSSION 15

CHAPTER 7 FUTURE SCOPE 17

CHAPTER 8 CONCLUSION 18

REFERENCES 19

LIST OF FIGURES

FIGURE 1 SUBSET BEFORE AND AFTER DEFORMATION. 1
FIGURE 2 RADIAL AND TANGENTIAL DISTORTION.
FIGURE 3 EFFECT OF RADIAL DISTORTION. 3
FIGURE 4 SAMPLE WITH SPECKLE PATTERN. 10
FIGURE 5 SETUP FOR IN-PLANE TRANSLATION TEST USING ZEISS SMARTZOOM 5 11
FIGURE 6 CONTOUR MAPS OF X AND Y DIRECTIONAL DISPLACEMENTS. 11
FIGURE 7 SETUP FOR IN-PLANE TRANSLATION TEST FOR CHEAP LENS. 11
FIGURE 8 CONTOUR MAPS OF X AND Y DIRECTIONAL DISPLACEMENTS. 11
FIGURE 9 SAMPLE USED IN DIC TESTER AND SAMPLE WITH SPECKLE PATTERN. 13
FIGURE 10 CONTOUR PLOT OF STRAINS FROM DIC BEFORE CORRECTION. 13
FIGURE 11 STRAIN DATA FROM ANSYS FOR DIC TESTER. 14
FIGURE 12 CONTOUR MAPS OF X AND Y DIRECTIONAL DISPLACEMENTS OF SAMPLE BEFORE DISTORTION CORRECTION. 15
FIGURE 13 PLOT COMPARING THE ERROR BEFORE AND AFTER CORRECTION. 15
FIGURE 14 CONTOUR PLOT OF STRAINS FROM DIC AFTER CORRECTION. 16
FIGURE 15 STRAIN DATA FROM ANSYS FOR DIC TESTER. 16

ABBREVIATIONS

DIC	Digital Image Correlation
GPR	Gaussian Process Regression
FWD	Free Working Distance

NOTATIONS

δr-Radial Distortion
δt-Tangential Distortion
x-coordinate of undistorted point
y-coordinate of undistorted point
x'-coordinate of distorted point
y'-coordinate of distorted point
$\propto_x$-amount of distortion in x direction
$\propto_y$-amount of distortion in y direction
$\propto_r$-amount of radial distortion
$k_1,\ k_2,\ k_3$-coefficients of radial distortion
r-radial distance
u'_x- displacements with the lens distortion in x direction
u'_y-displacements with the lens distortion in y direction
u_x- displacements without the lens distortion in x direction
u_y-displacements without the lens distortion in y direction
x'_u-coordinates of a point before deformation with the lens distortion in x direction
y'_u-coordinates of a point before deformation with the lens distortion in y direction
x'_d-coordinates of a point after deformation with the lens distortion in x direction
y'_d-coordinates of a point after deformation with the lens distortion in y direction
x_u- coordinates of a point before deformation without the lens distortion in x direction
y_u- coordinates of a point before deformation without the lens distortion in y direction
x_d-coordinates of a point after deformation without the lens distortion in x direction
y_d-coordinates of a point after deformation without the lens distortion in x direction
$\propto_{xu}$- x component of the lens distortion at the point x_u
$\propto_{yu}$- y component of the lens distortion at the point y_u
$\propto_{xd}$- x component of the lens distortion at the point x_d
$\propto_{yd}$- y component of the lens distortion at the point y_d
$a_1,\ a_2,\ a_3,\ b_1,\ b_2,\ b_3$-coefficients that represent the in-plane translation.

CHAPTER 1 INTRODUCTION

1.1. INTRODUCTION TO DIC

Digital Image Correlation (DIC) is an effective and practical tool for full-field deformation measurement, which has been commonly accepted and widely used in the field of experimental mechanics. Recently, the fundamental principles of DIC technique have been systematically reviewed and introduced in a review paper written by the author of this paper. However, several basic problems of DIC still remain unclear to us, and the DIC technique can also been improved in terms of robustness and computational efficiency. This work reports several important advances we recently made on DIC technique, which can be regarded as important and beneficial supplements to the recent review paper. In essence, DIC is an image-based deformation measuring technique based on digital image processing and numerical computation. In the most widely used subset based DIC technique, a reference square subset with sufficient intensity variations is selected from the reference image (or source image). Then, by means of a predefined criterion and a certain optimization algorithm, the DIC technique searches the deformed image for the deformed (or target) subset, whose intensity pattern is of maximum similarity (or minimum difference) with the reference subset. The differences between the reference subset and the target subset yield the subset center's displacement. vector. To obtain reliable and accurate matching, the selected subset must contain sufficient intensity variations to ensure that it can be uniquely and accurately identified in the deformed image, which means that the test object surface has to be covered with natural or artificial speckle pattern (or more exactly, random gray level intensity variation). The speckle pattern deforms together with the specimen surface during deformation and will be further used as a faithful carrier of surface deformation information in the subsequent matching process of DIC.

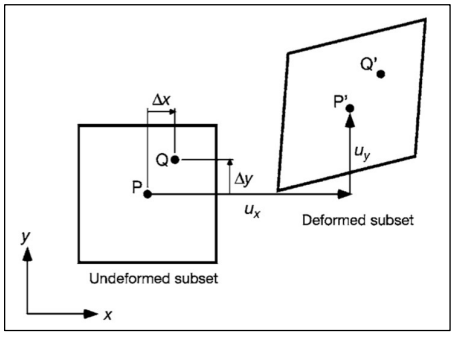

Figure 1 Subset before and after deformation.

Optical deformation measurements with DIC are widely used for the measurement of displacement and strain in the field of experimental solid mechanics. DIC can be used to obtain the surface displacement by comparison of digital images of undeformed and deformed configurations. Since the experimental setup is simple and the requirement from the measurement environment is low, the measurement can be performed simply and easily. In addition, digital image correlation does not require phase analysis of fringe patterns and it is easy to realize automation of the measurement process. Therefore, the digital image correlation method has been widely accepted and commonly used as a powerful tool for surface deformation measurement on the macroscale and microscale. For macroscale deformation measurement with digital image correlation, camera lenses, such as a fixed-length lens or a zoom lens, etc., are often used for speckle-image recording with a certain magnification.

1.2. DISTORTIONS AND ITS EFFECTS

Image distortions are unavoidably introduced due to lens aberrations, which may corrupt the real displacement induced by external loading and minimize the measurement accuracy. However, a relatively small distortion is found when a macroscale measurement is performed with the DIC; so, macroscale distortion can be practically ignored. Recently, with the development of modern micromachining technology, devices have become more and more miniaturized, and there is a growing interest in measuring the structural behavior on the microscale. For microscale deformation measurement with digital image correlation, a microscope is often used for high-resolution imaging. For example, researchers measured the residual stress and the deformation caused by the residual stress of a MEMS film by means of DIC and an ultra-depth microscope. Usually, the object needs to be close to the lens when a 2D DIC is used for microscale deformation measurement at high magnification. According to the pinhole camera model, there is an increasing potential for image distortion for the quantitative measurement. Therefore, image distortion must be corrected for microscale deformation measurement at a high magnification to ensure measurement accuracy.

Lens distortion can be divided into tangential distortion and radial distortion. Radial distortion (δr) is caused by the radial curvature change of an optical lens, and tangential distortion (δt) is caused by tangential deformation perpendicular to the radial direction. Generally, radial distortion is much larger than tangential distortion, so the influence of tangential distortion is generally not considered. A simple linear least-

squares algorithm to estimate the distortion coefficient from the distorted displacement results for a rigid body, in-plane translation tests, which can be used to correct the distorted displacement fields to obtain unbiased displacement and strains fields. The purpose of the project is to investigate the distortion correction of a microscopy lens for quantitative measurements with high accuracy. Microscale speckle patterns are used as calibrated references for lens distortion correction, and the results are compared. First, lens distortion correction based on a first-order warping function is analyzed and methodology for the distortion coefficient is established based on digital image. Rigid body, in-plane translation tests of the micro-speckle pattern are performed. Finally, lens distortion is corrected by digital image correlation, which is followed by discussion of the compared results.

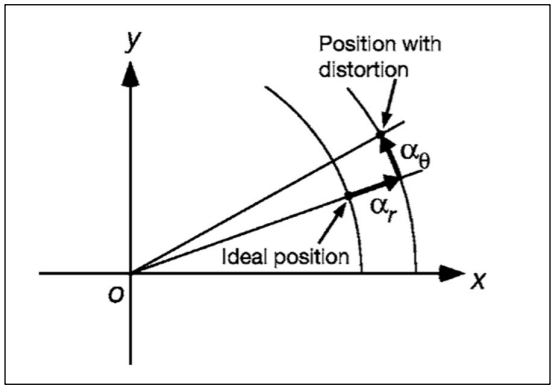

Figure 2 Radial and tangential distortion.

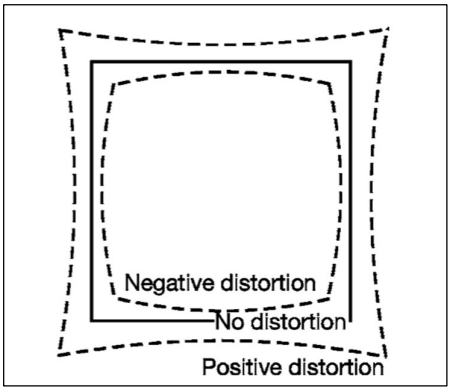

Figure 3 Effect of radial distortion.

1.3. OBJECTIVES

A simple method of lens distortion correction is proposed in order to improve the measurement accuracy of digital image correlation for two-dimensional displacement measurement. The effectiveness of the proposed method is demonstrated by applying it to an in-plane translation test and tension tests. The experimental results show that the proposed distortion correction method eliminates the effect of lens distortion from measured displacements.

CHAPTER 2 LITERATURE REVIEW

2.1. INTRODUCTION

Digital Image Correlation (DIC) is a powerful, non-contact optical method used to measure deformation, strain, and displacement in materials. Due to its high accuracy, flexibility, and ease of use, DIC has found widespread application in various fields of material science and engineering. This literature review summarizes significant contributions to the development and application of DIC.

2.2. EARLY APPLICATIONS AND METHODOLOGICAL DEVELOPMENTS

- **Lord, Penn, and Whitehead (2008)**

  This study was one of the early works that showcased the potential of DIC for improving measurement accuracy in residual stress analysis. The researchers successfully integrated DIC with the incremental hole-drilling method, highlighting its ability to capture detailed strain data, which is crucial for precise stress analysis.

2.3. INNOVATIONS IN DIC TECHNOLOGY

- **Arabul and Lunt (2022)**

  The introduction of a novel, low-cost DIC-based residual stress measurement device by Arabul and Lunt marked a significant innovation. This device makes high-precision measurement techniques more accessible, enabling broader application in various fields. The study demonstrated the effectiveness of the DIC-based device in accurately measuring residual stress, paving the way for more cost-effective solutions in industrial applications.

- **Barile et al. (2023)**

  Barile and colleagues implemented Gaussian Process Regression (GPR) to enhance the analysis of strain data obtained from DIC. This methodological advancement provides a more robust statistical framework for interpreting DIC data, improving the accuracy and reliability of strain measurements.

2.4. APPLICATION IN VARIOUS MATERIALS AND CONDITIONS

- **Peng et al. (2019)**

  Peng and his team explored the application of DIC in conjunction with the hole-drilling method for in-situ residual stress measurement. Their work emphasized the real-time monitoring capabilities of DIC, which is crucial for dynamic testing environments and complex material systems.

- **Singh and Shukla (2014)**

  This study applied DIC to measure residual stress in polymers, demonstrating the method's versatility. By accurately capturing the deformation patterns in polymers, DIC provided insights into the material's behaviour under various loading conditions.

2.5. ADDRESSING METHODOLOGICAL CHALLENGES

- **Sayers and Dahm (2011)**

  The researchers applied DIC to hole-drilling residual stress measurements in pipelines. Their study addressed challenges such as stress concentration factors and drilling parameters, highlighting DIC's capability to provide accurate and detailed strain measurements even in challenging conditions.

- **Cho and Lee (2002)**

  Cho and Lee used DIC in combination with the boundary element method to measure residual stress in welded parts. Their work showcased the ability of DIC to accurately capture stress distribution and deformation in complex welded structures.

2.6. RECENT DEVELOPMENTS AND FUTURE DIRECTIONS

- **Peng, Zhao, Chen, and Dong (2019)**

  The combination of blind-hole drilling and DIC for residual stress measurement in steel structures was explored in this study. It demonstrated DIC's effectiveness in providing detailed strain maps, enhancing the understanding of stress distribution in structural materials.

- **Huber, Pippan, and Weiss (2006)**

  This study evaluated the integral method for residual stress determination using DIC, showing how advanced analytical techniques can be integrated with DIC to improve measurement accuracy.

CHAPTER 3 DISTORTION CORRECTION BY MEASURING RIGID BODY DISPLACEMENT

3.1. DISTORTION MODEL

The image distortion model is usually given as a mapping from the distorted image coordinates to the undistorted image coordinates. The coordinates x′ and y′ of a point on a distorted image can be expressed as

$$x' = x + \propto_x,$$

$$y' = y + \propto_y,$$

(1)

where x and y are the distortion-free image coordinates and $\propto_x$ and $\propto_y$ express the amounts of lens distortion along the x and y directions, respectively. The image distortion model can be decomposed into two terms, namely, radial distortion and tangential distortion. As shown in Fig. 2, radial distortion is a deformation of an image along the direction from the centre of distortion to the considered point. On the other hand, tangential distortion is a deformation perpendicular to this direction. It is found that for many applications, tangential distortion need not be considered, its amount is very small compared with that of radial distortion. Figure 3 shows the effect of radial distortion. Radial distortion causes an inward or outward displacement of a given image point from its ideal location as shown in this figure. Negative radial displacement of the image points is referred to as barrel distortion; positive radial displacement is referred to as pincushion distortion. This type of distortion is strictly symmetric about the optical axis. Because digital image correlation detects displacements directly from images as described in the previous section, the distortion of images shown in Fig. 3 greatly affects the measured displacements.

The amount of radial distortion $\propto_r$ can be expressed in the following form:

$$\propto_r = k_1 r^3 + k_2 r^5 + k_3 r^7 + \cdots,$$

(2)

where r is the radial distance from the centre of the distortion to the image points, and k_1, k_2, k_3 are the coefficients of the radial distortion. Assuming that the terms of higher order than 3 are negligible, Eq. (4) can be rewritten as

$$\propto_r = k_1 r^3 \tag{3}$$

At each image point represented by polar coordinates, the radial distortion corresponds to the distortion along the radial direction. The image point can also be expressed in terms of Cartesian coordinates. Then, the amount of the radial distortion can be represented by

$$\propto_x = k_1 x(x^2 + y^2)$$

$$\propto_y = k_1 y(x^2 + y^2) \tag{4}$$

It is seen from Eq. (3) and (4) that the amount of the distortion is proportional to the cube of the radial distance r. Thus, the distortion can be corrected by knowing the coefficient k_1.

When decentring distortion and thin-prism distortion are present, tangential distortion should be considered for the distortion correction. In this project, however, only radial distortion is considered, because, as previously mentioned, the effect of tangential distortion is much smaller.

3.2. DISTORTION CORRECTION

When an optical system with lens distortion is used for in-plane displacement measurement with digital image correlation, the displacements u'_x and u'_y with the lens distortion can be expressed using Eqs. (1) and (4) as

$$\begin{aligned} u'_x = x'_d - x'_u &= (x_d + \propto_{xd}) - (x_u + \propto_{xu}) = x_d - x_u + \propto_{xd} - \propto_{xu} \\ &= u_x + k_1[x_d(x_d^2 + y_d^2) - x_u(x_u^2 + y_u^2)], \end{aligned}$$

$$u'_y = y'_d - y'_u = \left(y_d + \propto_{yd}\right) - \left(y_u + \propto_{yu}\right) = y_d - y_u + \propto_{yd} - \propto_{yu}$$
$$= u_y + k_1[y_d(x_d^2 + y_d^2) - y_u(x_u^2 + y_u^2)],$$

(5)

where x'_u and y'_u are the coordinates of a point before deformation with the lens distortion, x'_d and y'_d are those after deformation, x_u and y_u are those of the distortion-free location of the point before deformation, and x_d and y_d are those after deformation. Finally, $\propto_{xu}$ and $\propto_{yu}$ are the x and y components of the lens distortion at the point (x_u, y_u), $\propto_{xd}$ and $\propto_{yd}$ are those at the point (x_d, y_d), and u_x and u_y are the displacement components without the lens distortion.

It is supposed that in-plane translation, rotation, or both tests are performed, and the displacements are measured by digital image correlation. The displacements u_x and u_y in Eq. (5) are constants within the image for the in-plane translation tests. For rotation tests or combined translation and rotation tests, they can be represented as two-dimensional plane surfaces. Therefore, the measured displacements of in-plane translation, rotation, or both can be represented as

$$u'_x = a_1 x_u + a_2 y_u + a_3 + k_1[x_d(x_d^2 + y_d^2) - x_u(x_u^2 + y_u^2)],$$

$$u'_y = b_1 x_u + b_2 y_u + b_3 + k_1[y_d(x_d^2 + y_d^2) - y_u(x_u^2 + y_u^2)],$$

(6)

where $a_1, a_2, a_3, b_1, b_2, b_3$ are coefficients that represent the in-plane translation. The displacements are obtained at the points given by the distorted coordinates. On the other hand, the distortion model is a function of the distortion-free coordinates. Therefore, the distortion coefficient k_1 and the other coefficients cannot be determined directly. Thus, the method of least squares with an iterative procedure is adopted for the determination of the coefficients in this study.

First, the coordinates x'_u, y'_u, x'_d, y'_d of the points with the lens distortion are substituted on the right-hand side of Eq. (6) instead of the distortion-free coordinates x_u, y_u, x_d, and y_d as initial values. Then, approximate values of the coefficients are determined in the least-squares sense as

$$g = (X^T X)^{-1} X^T b,$$

(7)

and x and b are given by,

$$\mathbf{x} = \begin{bmatrix} x_{d1}(x_{d1}^2+y_{d1}^2)-x_{u1}(x_{u1}^2+y_{u1}^2) & x_{u1} & y_{u1} & 1 & 0 & 0 & 0 \\ x_{d2}(x_{d2}^2+y_{d2}^2)-x_{u2}(x_{u2}^2+y_{u2}^2) & x_{u2} & y_{u2} & 1 & 0 & 0 & 0 \\ \vdots & \vdots & \vdots & \vdots & \vdots & \vdots & \vdots \\ x_{dn}(x_{dn}^2+y_{dn}^2)-x_{un}(x_{un}^2+y_{un}^2) & x_{un} & y_{un} & 1 & 0 & 0 & 0 \\ y_{d1}(x_{d1}^2+y_{d1}^2)-y_{u1}(x_{u1}^2+y_{u1}^2) & 0 & 0 & 0 & x_{u1} & y_{u1} & 1 \\ y_{d2}(x_{d2}^2+y_{d2}^2)-y_{u2}(x_{u2}^2+y_{u2}^2) & 0 & 0 & 0 & x_{u2} & y_{u2} & 1 \\ \vdots & \vdots & \vdots & \vdots & \vdots & \vdots & \vdots \\ y_{dn}(x_{dn}^2+y_{dn}^2)-y_{un}(x_{un}^2+y_{un}^2) & 0 & 0 & 0 & x_{un} & y_{un} & 1 \end{bmatrix} \quad (8)$$

$$b^T = [u'_{x1} \quad u'_{x2} \quad \cdots \quad u'_{xn} \quad u'_{y1} \quad u'_{y2} \quad \cdots \quad u'_{yn}]$$

where the subscript 1,2, ..., n represents the indices of the data points and n is the total number of the data points. In the cases that the centre of the distortion deviates from the centre of the image or the centre of the distortion cannot be known in advance, the unknown coordinate of the centre of the distortion is substituted for the coordinates in the preceding equations. Then, a nonlinear least-squares method is used to obtain the coefficients. Next, the approximate coordinates x_u, y_u, x_d, and y_d of the points without the lens distortion are calculated using the approximate value of the coefficient k_1. Then, the approximate coordinates are used for the recalculation of the coefficients. This procedure is repeated until the coefficients, and the coordinates are converged. Finally, the distortion coefficient k_1 is obtained by adopting the convergent value. Usually about four or five iterations are needed to get the convergent values.

Using the coefficient k_1, the amounts of the distortion $\propto_{xu}$, $\propto_{yu}$, $\propto_{xd}$, and $\propto_{yd}$ are determined, and the displacements ux and uy without the lens distortion are obtained from the corrected coordinates x_u, y_u, x_d, and y_d. Here, the iterative procedure is again used to determine the corrected coordinates x_u, y_u, x_d, and y_d from the distorted coordinates x'_u, y'_u, x'_d, and y'_d.

CHAPTER 4 SAMPLE PREPARATION

DIC uses a correlation algorithm to obtain the displacements by identifying areas of matching grey scale values between the speckle pattern in each subset of the deformed and undeformed images. The position where the correlation function value is maximised in the deformed image corresponds to the movement of the pattern during deformation. To facilitate the correlation a stochastic speckle pattern is applied to the specimen surface to provide random grey level variations, the quality of which is fundamental to the precision of the measured displacement data. Spatial resolution of the data is maximised by reducing the size of the subsets, but as the interrogation cell size decreases, the uncertainty in the strain measurement increases due to a reduction in the number of features to track within the subset.

It is desirable to have a pattern with high levels of unique features and randomness to maximise the correlation function response when a match is found in each interrogation cell. This reduces the uncertainty in matching the pattern from image to image. Therefore, the quality of the speckle pattern has a large influence on the correlation function values created for areas of similar patterns, and hence the accuracy of the calculated displacements.

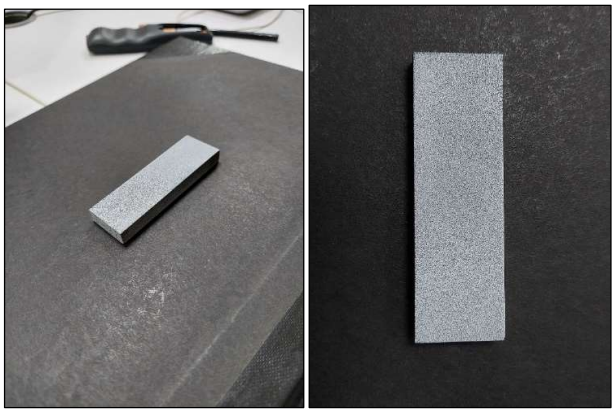

Figure 4 Sample with speckle pattern.

A steel sample plate cut into 72mm x 23mm using Wire Electrical Discharge Machining was used. The sample was polished using a 250-grade polishing paper, 600-grade, and 1000-grade polishing paper in succession.

Then a random speckle like pattern was laid onto the polished surface using spray cans. First, a uniform layer of white matte paint was sprayed on the polished surface. After this layer was dried black matte paint was sprayed from afar to create a fine and dense speckle pattern. Figure 4 shows the fine speckle pattern.

CHAPTER 5 EXPERIMENTAL SETUP

5.1. RIGID BODY IN-PLANE TRANSLATION TEST FOR EXPENSIVE LENS

A rigid body translation test was performed using Zeiss SmartZoom 5 microscope. The sample was kept parallel to the edges of the bed under the ring lights of the microscope. A PlanApo D 0.5x/0.03 FWD 78mm lens was used, with digital zoom set at 30x, to capture images.

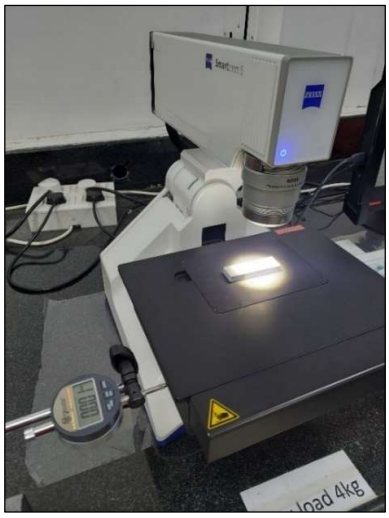

Figure 5 Setup for in-plane translation test using Zeiss SmartZoom 5

A dial gauge was used to measure the displacement accurately. Images were captured for displacement of 0.5mm in x direction.

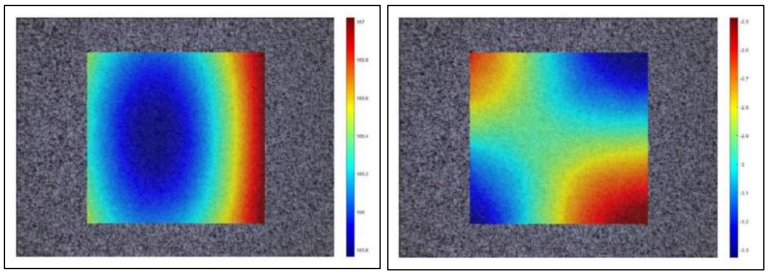

Figure 6 Contour maps of x and y directional displacements of sample.

Analysing these plots shows that there is significant lens distortion at the edges of the images and less distortion in the middle of the image, which is expected.

5.2. RIGID BODY IN-PLANE TRANSLATION TEST FOR CHEAP LENS

A rigid body translation test was performed on a HASS 1000S 5-axis Hybrid UMC. The sample was held in a vice with top face parallel to the camera sensor. A 100X Zoom Lens with a Raspberry Pi Camera lens was used to capture images. The machine precisely translated for 2mm with increments of 0.5mm in x direction.

Figure 7 Setup for in-plane translation test for cheap lens.

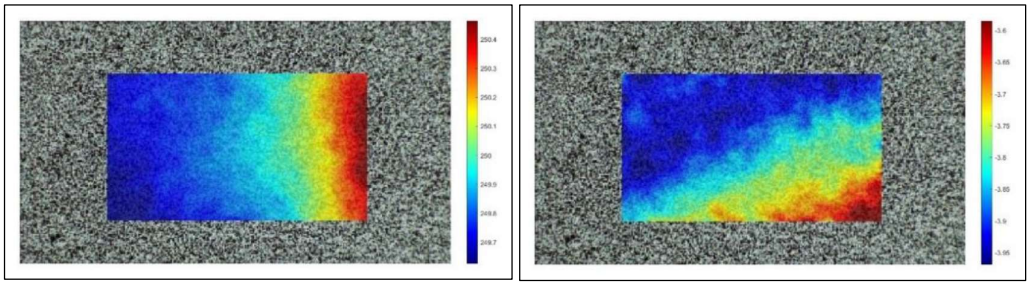

Figure 8 Contour maps of x and y directional displacements of sample.

5.3. TEST TO COMPARE DIC TO FEM ANALYSIS (DIC Tester)

The sample was made from maraging steel plate cut into shape using Wire-Electric Discharge Machining. A clamp was used to pinch the ends, as shown in Figure 10 of the sample to produce strain. There would be compression on the bottom side of

the curve of the sample and tension on the top part of the sample. As this test was performed just to compare DIC with a FEM model to prove that the proposed method to correct distortion has the same increase in accuracy for a real-life example.

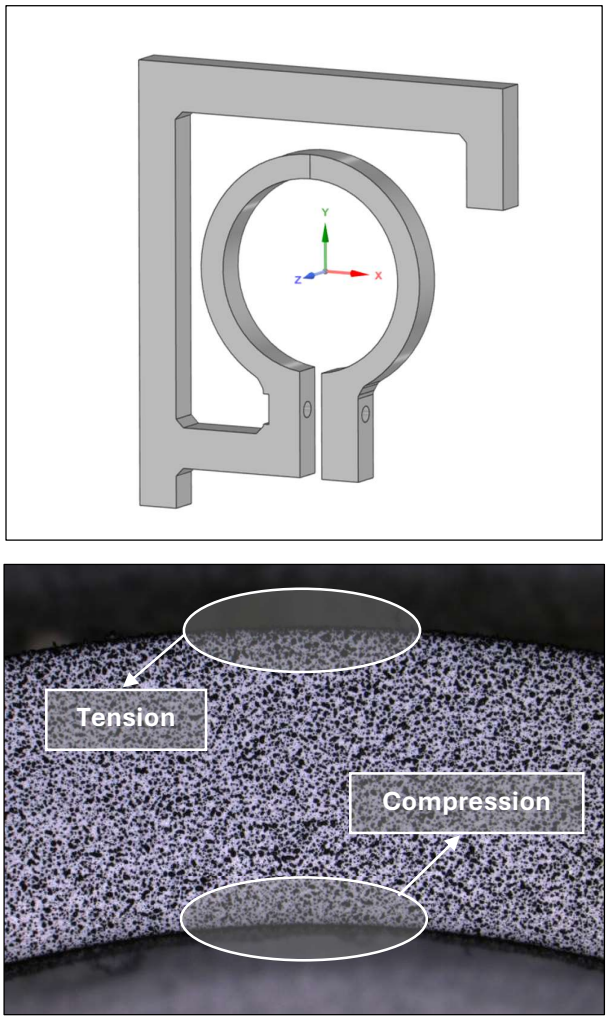

Figure 9 Sample used in DIC Tester and sample with speckle pattern.

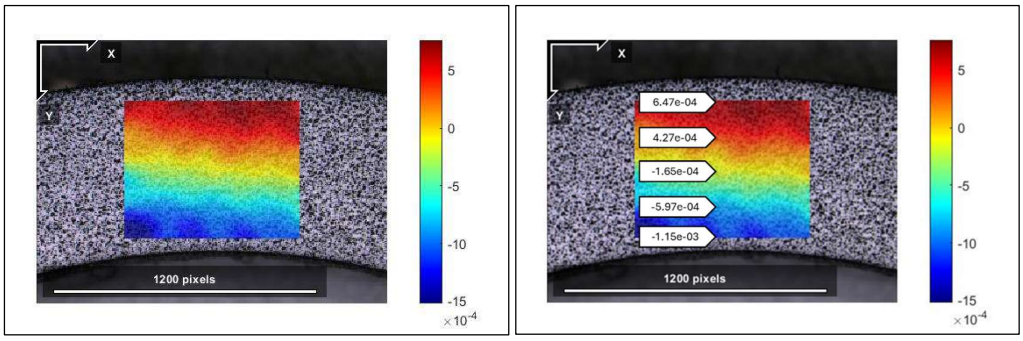

Figure 10 Contour plot of strains from DIC before correction.

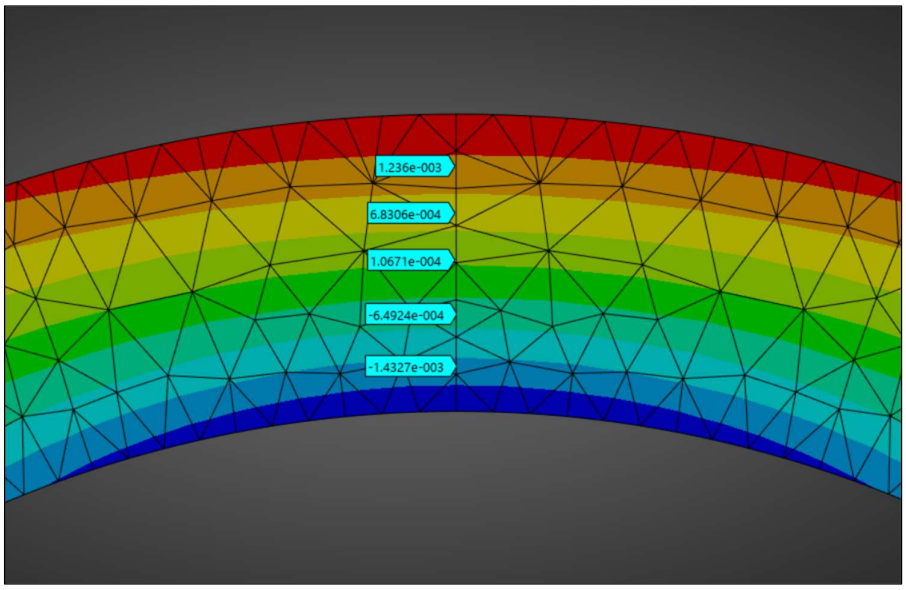

Figure 11 Strain data from Ansys for DIC tester.

The data obtained from DIC without accounting for distortion correction is not accurate. The contour from Figure 8 shows that the strains are not properly distributed and the tension is concentrated at one corner and compression on the other corner of the plot. This varition in the results is the sole reason for correcting distortion.

CHAPTER 6 RESULTS AND DISCUSSION

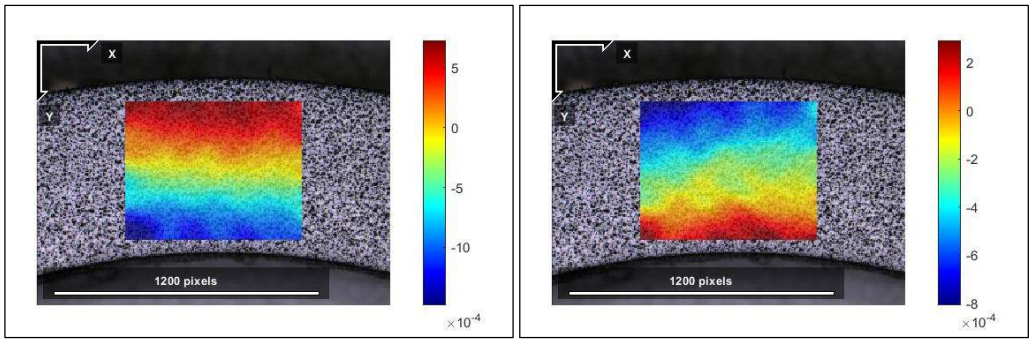

Figure 12 Contour maps of x and y directional displacements of sample after distortion correction.

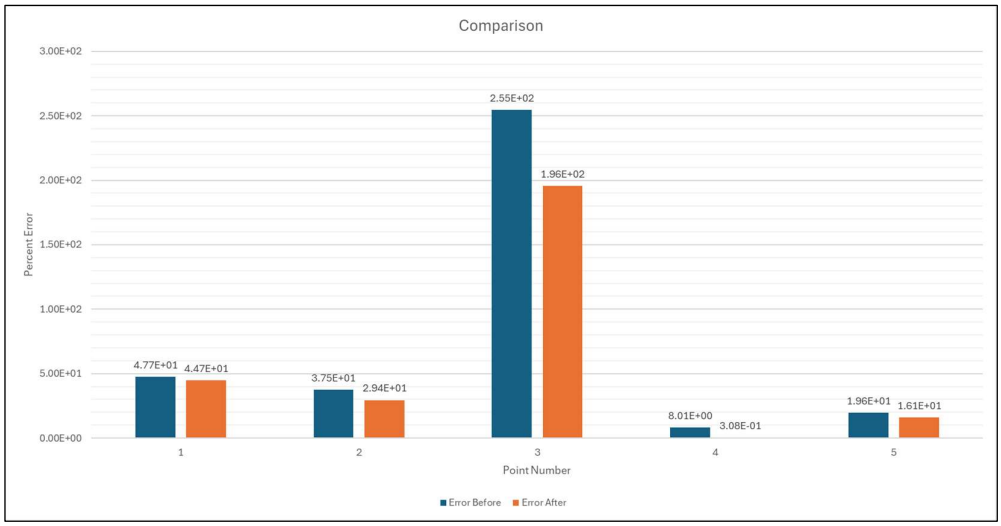

Figure 13 Plot comparing the error before and after correction.

The displacements for the DIC tester were corrected by the proposed method. Figure 12 shows the corrected distribution of the displacements shown in Figure 6. Almost uniform displacement distributions are obtained. This proves that the proposed method is effective as the error reduction in displacements is around 20%. Figure 13 shows the plots for displacements before and after correction, it is clear that the data obtained after correction is more reliable than the data obtained before correction.

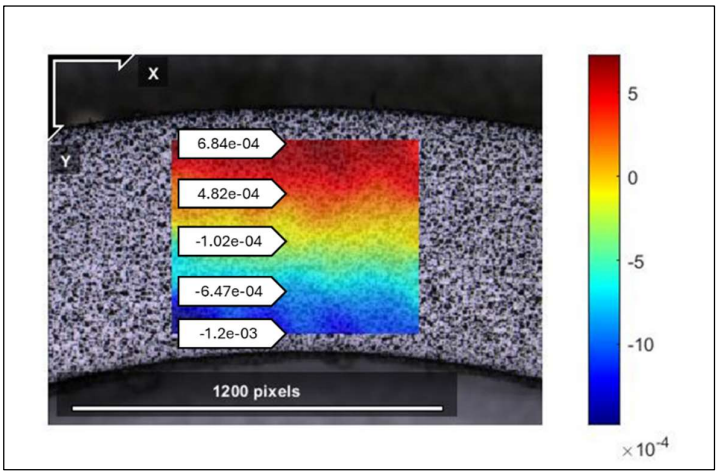

Figure 14 Contour plot of strains from DIC after correction.

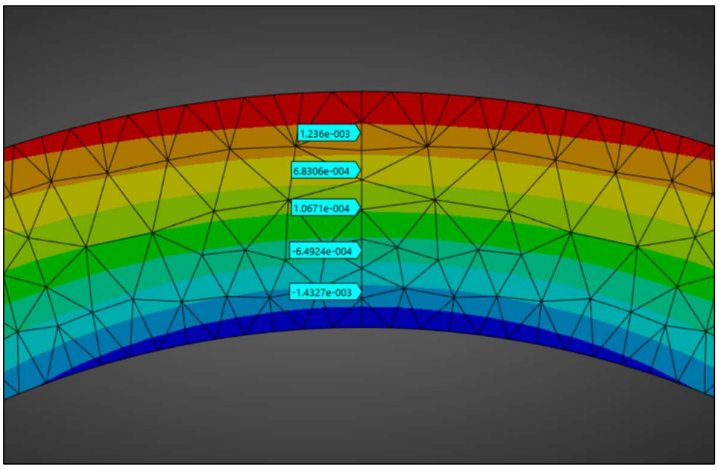

Figure 15 Strain data from Ansys for DIC tester.

The results shown in Figure 14 shows that the strains are much more accurate than without correcting. However, as it was not possible to match each point from DIC with Ansys but, the points are close and are comparable.

CHAPTER 7 FUTURE SCOPE

- Calculating the corrected displacements for the cheap lens setup.
- Comparing the obtained results with the FEM model.
- Comparing them with the results from expensive lens setup.
- Analysing if a accurate DIC setup can be developed using cost-effective lens.

CHAPTER 8 CONCLUSION

- Displacement measurement using digital image correlation with lens distortion correction has been described.
- The lens distortion can be measured by the displacements obtained in in-plane translation tests.
- Then, the lens distortion in the measurement results of the displacement can be corrected by the proposed method. The method does not need any calibration patterns or subsequent image processing such as the detection of targets and straight lines.
- Thus, the correction procedure becomes simple and easy. As a result, an optical system with distortion, such as a low-cost camera system and a zoom lens, can be utilized in the measurements.

REFERENCES

1. Sicot, O., Gong, X. L., Cherouat, A., & Lu, J. (2004). Influence of experimental parameters on determination of residual stress using the incremental hole-drilling method. Composites Science and Technology, 64(2), 171-180. https://doi.org/10.1016/S0266-3538(03)00278-1

2. Nelson, D. V. (2010). Residual stress determination by Hole drilling combined with optical methods. Experimental Mechanics, 50(2), 145-158. https://doi.org/10.1007/s11340-009-9329-3

3. Nau, A., & Scholtes, B. (2013). Evaluation of the High-Speed Drilling Technique for the Incremental Hole-Drilling Method. Experimental Mechanics, 53(4), 531-542. https://doi.org/10.1007/s11340-012-9641-1

4. ASTM International. (2020). Standard Test Method for Determining Residual Stresses by the Hole-Drilling Strain-Gage Method 1. ASTM E837. https://doi.org/10.1520/E0837-20

5. Hagara, M., & Pástor, M. (2021). A complex review of the possibilities of residual stress analysis using moving 2D and 3D digital image correlation system. Strojnicky Casopis, 71(1), 61-78. https://doi.org/10.2478/scjme-2021-0006

6. Lord, J. D., Penn, D., & Whitehead, P. (2008). The application of digital image correlation for measuring residual stress by incremental hole drilling. Applied Mechanics and Materials, 13-14, 65-73. https://doi.org/10.4028/www.scientific.net/AMM.13-14.65

7. Arabul, E., & Lunt, A. J. G. (2022). A Novel Low-Cost DIC-Based Residual Stress Measurement Device. Applied Sciences (Switzerland), 12(14). https://doi.org/10.3390/app12147233

8. Niku-Lari, A., Lu, J., & Flavenot, J. F. Measurement of Residual-Stress Distribution by the Incremental Hole Drilling Method.

9. Peng, Y., Zhao, J., Chen, L., & Dong, J. (2021). Residual stress measurement combining blind-hole drilling and digital image correlation approach. Journal of Constructional Steel Research, 176. https://doi.org/10.1016/j.jcsr.2020.106346

10. Penn, D., & Whitehead, P. (2008). The application of digital image correlation for measuring residual stress by incremental hole drilling. Applied Mechanics and Materials, 13-14, 65-73. https://doi.org/10.4028/www.scientific.net/AMM.13-14.65

11. Arabul, E., & Lunt, A. J. G. (2022). A Novel Low-Cost DIC-Based Residual Stress Measurement Device. Applied Mechanics and Materials, 12(14). https://doi.org/10.3390/app12147233

12. Barile, C., Carone, S., Casavola, C., & Pappalettera, G. (2023). Implementation of Gaussian Process Regression to strain data in residual stress measurements by hole drilling. Measurement, 211. https://doi.org/10.1016/j.measurement.2023.112590

13. Stefanescu, D., Truman, C. E., Smith, D. J., & Whitehead, P. S. (2006). Improvements in Residual Stress Measurement by the Incremental Centre Hole Drilling Technique. Experimental Mechanics, 46(4), 417-427. https://doi.org/10.1007/s11340-006-7686-8

14. Peng, Y., Zhao, J., Chen, L., & Dong, J. (2019). DIC-hole drilling method for in-situ residual stress measurement. Journal of Constructional Steel Research, 275. https://doi.org/10.1051/matecconf/201927502004

15. Steinzig, M., & Rasty, J. (2011). Influence of drilling parameters on the accuracy of hole-drilling residual stress measurements. Conference Proceedings of the Society for Experimental Mechanics Series, 8, 95-109. https://doi.org/10.1007/978-1-4614-0225-1_12/COVER

16. Sato, Y., Fukuoka, T., Nakashima, H., & Maruyama, K. (1996). Stress calculation error analysis for incremental hole-drilling residual stress measurements. Journal of Engineering Materials and Technology, Transactions of the ASME, 118(1), 120-126. https://doi.org/10.1115/1.2805924

17. Huber, N., Pippan, R., & Weiss, B. (2006). Evaluation of the Integral Method for the Determination of Residual Stresses by Incremental Hole-Drilling Part 2. Experimental Mechanics, 46(3), 297-304. https://doi.org/10.1007/s11340-006-5872-8

18. Mahnken, R., Kuhl, D., & Tschentscher, A. (2019). Measurement of residual stresses by means of the incremental hole-drilling method: validation, comparison and modelling. Measurement, 131, 383-395. https://doi.org/10.1016/j.measurement.2018.08.021

19. Cho, Y., & Lee, D. (2002). Accurate measurement of residual stress for welded parts using ESPI hole drilling and the boundary element method. Optics and Lasers in Engineering, 37(4), 321-334. https://doi.org/10.1016/S0143-8166(01)00076-8

20. Korsunsky, A. M., & Gill, J. (2010). Study of the residual stress and distortion in structural steel welded plates by the incremental hole-drilling method. Materials Science Forum, 652, 207-212. https://doi.org/10.4028/www.scientific.net/MSF.652.207

21. Beghini, M., Bertini, L., & Santus, C. (2008). Residual stress measurements by the incremental hole-drilling method: effect of plasticity. Experimental Mechanics, 48(5), 581-588. https://doi.org/10.1007/s11340-007-9111-8

22. Santos, R. A., & Nunes, M. (2015). Residual stress measurements in steel and aluminium by the incremental hole drilling technique. Procedia Engineering, 114, 175-182. https://doi.org/10.1016/j.proeng.2015.08.073

23. Rossini, N. S., Dassisti, M., & Benyounis, K. Y. (2010). Methods of measuring residual stresses in components. Materialwissenschaft und Werkstofftechnik, 41(6), 501-512. https://doi.org/10.1002/mawe.201000542

24. Deng, D., Lindgren, L. E., & Niu, L. (2006). Determination of residual stress in inhomogeneous materials using incremental hole-drilling and DIC. Experimental Mechanics, 46(1), 123-132. https://doi.org/10.1007/s11340-006-5863-9

25. Sayers, C. M., & Dahm, K. L. (2011). Application of digital image correlation to hole-drilling residual stress measurements in pipelines. Journal of Pressure Vessel Technology, 133(6). https://doi.org/10.1115/1.4003749

26. Zhao, Y., Wang, H., & Yang, X. (2014). Incremental hole-drilling for residual stress measurement in an aircraft fuselage panel. Theoretical and Applied Fracture Mechanics, 70, 37-45. https://doi.org/10.1016/j.tafmec.2014.03.001

27. Mann, C. R., & Tuttle, T. W. (1998). Measurement of residual stresses in polymer-matrix composites by the incremental hole-drilling method. Journal of Composite Materials, 32(7), 662-680. https://doi.org/10.1177/002199839803200703

28. Peng, Z., Liu, Q., & Yu, J. (2017). In-situ residual stress measurement using digital image correlation and incremental hole-drilling. Experimental Techniques, 41(3), 279-288. https://doi.org/10.1007/s40799-016-0107-5

29. Lin, Z., & Sheng, L. (2018). Determination of residual stress distribution in functionally graded materials by the incremental hole-drilling method. Journal of Materials Research and Technology, 7(4), 396-405. https://doi.org/10.1016/j.jmrt.2018.02.007

30. Zhang, H., & Zhang, Z. (2019). Incremental hole-drilling and ESPI methods for residual stress measurement in multilayer materials. Materials Research Express, 6(7). https://doi.org/10.1088/2053-1591/ab1b2c

31. Singh, J., & Shukla, A. (2014). Measurement of residual stress in polymers by the incremental hole-drilling method using digital image correlation. Polymer Testing, 35, 66-74. https://doi.org/10.1016/j.polymertesting.2014.02.001

32. Zhang, Y., & Liu, S. (2010). Study on residual stress of welded joints using incremental hole-drilling and X-ray diffraction. Applied Mechanics and Materials, 29-32, 1666-1670. https://doi.org/10.4028/www.scientific.net/AMM.29-32.1666

33. Hart, G. W., & Hosseinzadeh, F. (2015). Incremental hole-drilling technique for measuring residual stress in metallic coatings. Journal of Thermal Spray Technology, 24(7), 1223-1231. https://doi.org/10.1007/s11666-015-0303-0

34. Sandig, J., & Richter, S. (2009). Incremental hole-drilling for residual stress measurement in thin coatings. Materials Science Forum, 638-642, 3200-3205. https://doi.org/10.4028/www.scientific.net/MSF.638-642.3200

35. Grum, J., & Slabe, J. M. (2006). Influence of heat treatment on residual stress distribution in high-speed steel analyzed by the incremental hole-drilling method. Journal of Materials Processing Technology, 173(3), 364-369. https://doi.org/10.1016/j.jmatprotec.2005.11.012

36. Nogueira, R. P., & Moya, J. E. (2012). Analysis of residual stress in injection-molded parts using the incremental hole-drilling method. Polymer Engineering & Science, 52(4), 835-842. https://doi.org/10.1002/pen.23089

37. Jones, C. R., & Taylor, D. (2010). Residual stress measurements in mechanical components by the incremental hole-drilling method. Engineering Failure Analysis, 17(2), 492-500. https://doi.org/10.1016/j.engfailanal.2009.09.005